NASA-CR-144874

(NASA-CR-144874) F-15 INLET ENGINE TEST TECHNIQUES AND DISTORTION METHODOLOGIES STUDIES. VOLUME 9: STABILITY AUDITS Final Report (McDonnell Aircraft Co.) 35 p HC A03/MF A01 CSCL 21E G3/07

N78-30131

Unclas 30408

F-15 Inlet/Engine Test Techniques and Distortion Methodologies Studies

Volume IX - Stability Audits

Contract Number NAS4-2364

NASA Contractor Report 144874

F-15 Inlet/Engine Test Techniques and Distortion Methodologies Studies

Volume IX - Stability Audits

C.H. Stevens
E.D. Spong
M.S. Hammock

McDonnell Douglas Corporation
McDonnell Aircraft Company
St. Louis, Missouri

Prepared for
Dryden Flight Research Center
under Contract NAS4-2364

National Aeronautics
and Space Administration

June 1978

FOREWORD

This report was prepared by the McDonnell Aircraft Company (MCAIR), a division of the McDonnell Douglas Corporation, St. Louis, Missouri for the National Aeronautics and Space Administration, Dryden Flight Research Center, Edwards, California. The study was performed under NASA Contract NAS4-2364, "F-15 Inlet/Engine Test Techniques and Distortion Methodologies Study." The work was performed from March 1977 through February 1978 with Mr. Jack Nugent (NASA/Dryden) as Program Monitor and Mr. Harvey Neumann (NASA/Lewis) as Technical Monitor. Special acknowledgement is due Mr. T. Putnam (NASA/Dryden) for his constructive criticisms and suggestions.

The effort at McDonnell Aircraft Company was conducted under the technical leadership of the Engineering Technology Division. In addition to the authors listed on the cover, other MCAIR personnel that made significant contributions to this program were Mr. Edward Smith, Mr. Lee Weltmer and Mr. Mark Sawyer. Special acknowledgement is due Mr. Hershel Sams for his reviews and suggestions.

Significant subcontract support was provided by Mr. Wayne Walter and Mr. Lew Hayward of Pratt & Whitney Aircraft (P&WA), Government Products Division, under the direction of Mr. Frank Thompson.

This report consists of nine volumes. Technical discussions of the program, results and Appendices A and B are presented in Volume I (NASA CR 144866). Appendices C through J are presented in Volume II through IX (NASA CR 144867-144874) which present the distortion analysis plots and the associated statistical functions used for the analyses.

1. Report No.	2. Government Accession No.	3. Recipient's Catalog No.
NASA CR-144874		

4. Title and Subtitle F-15 Inlet/Engine Test Techniques and Distortion Methodologies Study

Volume IX - Stability Audits

5. Report Date
June 1978

6. Performing Organization Code

7. Author(s)

C. H. Stevens, E. D. Spong, M. S. Hammock

8. Performing Organization Report No.

9. Performing Organization Name and Address

McDonnell Aircraft Company
McDonnell Douglas Corporation
St. Louis, Missouri 63166

10. Work Unit No.
514-54-04

11. Contract or Grant No.
NAS4-2364

13. Type of Report and Period Covered
Contractor Report - Final

12. Sponsoring Agency Name and Address

National Aeronautics and Space Administration
Washington, DC 20546

14. Sponsoring Agency Code

15. Supplementary Notes

Program Monitor: Jack Nugent (NASA/Dryden)
Technical Monitor: Harvey Neumann (NASA/Lewis)

16. Abstract

The Stability Audit plots contained in this volume of the F-15 Inlet/Engine Test Techniques and Distortion Methodologies Study were used in accomplishing the primary study goal of determining if peak distortion data taken from a subscale inlet model can be used to predict peak distortion levels for a full scale flight test vehicle. The results of this study are contained in the Technical Discussion, Volume I (NASA CR 144866).

17. Key Words (Suggested by Author(s))		18. Distribution Statement
Compatibility	Scale Effects	Unclassified - Unlimited
Inlet/Engine Compatibility		
Reynolds Number		Star Category: 07
Frequency Content		
Engine Effects		
Stability Audit		

19. Security Classif (of this report)	20. Security Classif (of this page)	21. No. of Pages	22. Price
Unclassified	Unclassified	25	*

*For sale by the National Technical Information, Springfield, VA 22161

TABLE OF CONTENTS

LIST OF ILLUSTRATIONS

SYMBOLS

	Description	Units
ALPHA	Aircraft angle of attack	degrees
ALT	Altitude	meters (feet)
AVG	Average.	
b, B	Radial Distortion Weighting factor	
BYPASS	Inlet bypass area.	sq. meters (sq. inches)
Beta	Aircraft angle of sideslip	degrees
CIVV	Compressor Inlet (Fan) Variable Vanes . . .	degrees
Deg	Degree	degree
ΔP_{t_2}	Fluctuating component of individual probe pressure at the engine face	
$(\Delta P_{t_2})_{rms}$	Root mean square of fluctuating pressure . .	kPa (PSIA)
DELTA3	Inlet third ramp angle relative to the Inlet Reference Line	degrees
$\Delta P_{t_{2.5H}}$	Fluctuating component of fan exit total pressure/engine stream	kPa (PSIA)
$\Delta P_{t_{2.5C}}$	Fluctuating component of fan exit total pressure/fan stream	kPa (PSIA)
$\frac{\Delta P}{P}$, D_2	Spatial Distortion = $[(P_{t_2})_{max} - (P_{t_2})_{min}]/\overline{P}_{t_2}$	
FLT, FLIGHT	Flight test data notation	
FSCP	Full Scale Cold Pipe (without engine) wind tunnel test data notation	
FSE	Full Scale with Engine wind tunnel test data notation	
HZ	Hertz.	hertz
I.D., IDENT	Identification	
K_{a_2}, KA2	Fan distortion descriptor = $K_\theta + b\ K_{ra_2}$ . .	
K_θ, KTHETA	Circumferential distortion	
K_{ra_2}, KRA2	Radial distortion.	

SYMBOLS (Continued)

	Description	Units
BKRA2	Radial distortion multiplied by radial distortion weighting factor.	
KC2	High compressor distortion descriptor. . . .	
KθSP	Circumferential distortion descriptor used to calculate the high compressor distortion descriptor.	
kPa	Pressure, Killopascals	Killopascals
M_o	Freestream Mach number	
MACH	Freestream Mach number	
MAX	Maximum.	
MIN	Minimum.	
No.	Number	
P_{t_2}	Individual probe engine face steady state pressure	kPa (PSIA)
$\overline{P_{t_2}}$	48 probe averaged engine face steady state pressure	kPa (PSIA)
$\overline{P}_{t_{25H}}$	Average high compressor face steady state pressure	kPa (PSIA)
P_{t_o}	Freestream total pressure.	kPa (PSIA)
PT2I	Individual probe time variant engine face pressure	kPa (PSIA)
$\overline{PT2I}$, $\overline{PI}$	48 probe averaged time variant engine face pressure	kPa (PSIA)
PI/PS	Ratio of time variant to steady state 48 probe averaged engine face pressure . . .	
PSIA	Pressure (Pounds per Square Inch Absolute) .	PSIA
Q, q	Dynamic pressure	kPa (PSIA)
Re. No.	Reynolds number	
RHO	Inlet first ramp angle relative to the Inlet Reference Line	degrees
RMS, rms	Root mean square.	
Sec	Second	second

SYMBOLS (Continued)

	Description	Units
Series VII	1/6th scale inlet wind tunnel test series data notation.	
Series VIII	1/6th scale inlet wind tunnel test series data notation	
T_{t_2}	Engine face total temperature	°K
$T_{t_{25H}}$	High compressor inlet (or fan exit) total temperature.	°K
Tu	Turbulence	
W2	Engine/Fan airflow	kg/sec (LB/sec)
WAT2	Corrected fan airflow = $W2\sqrt{\theta_{t_2}}/\delta_{t_2}$	kg/sec (LB/sec)
WAT2 Design	Design corrected fan airflow	98.43 kg/sec (217 LB/sec)
WAT2 Percent	WAT2 divided by WAT2 Design x 100	
W25H	High compressor airflow	kg/sec (LB/sec)
WAT25H	Corrected high compressor airflow $W25H \sqrt{\theta_{t_{25H}}}/\delta_{t_{25H}}$	kg/sec (LB/sec)
WAT25H Design	Design corrected high compressor airflow . .	24.69 kg/sec (54.44 LB/sec)
WAT25H Percent	WAT25H divided by WAT25H Design x 100. . . .	
α	Aircraft angle of attack	degrees
β	Aircraft angle of sideslip	degrees
Δ_3	Inlet third ramp angle relative to the Inlet Reference Line	degrees
δ_{t_2}	Corrected average engine face total pressure $\overline{P}_{t_2}/101$	
$\delta_{t_{25H}}$	Corrected average engine face total pressure $\overline{P}_{t_{25H}}/101$	
ρ	Inlet first ramp angle relative to the Inlet Reference Line	degrees
σ	Standard deviation of the instantaneous pressure	kPa (PSIA)

	Description	Units
$\sigma_{xy}(\tau)$	Covariance of pressure data from probes x and y at lag time τ	kPa (PSIA)
$\sigma_{xy}(\tau=0)$	Covariance of pressure data from probes x and y at lag time $\tau=0$	kPa (PSIA)
θ_{t_2}	Corrected average engine face total temperature $T_{t_2}/288.15$	
$\theta_{t_{25H}}$	Corrected average high compressor face total temperature $T_{t_{25H}}/288.15$	

SUMMARY

Recent emphasis on increased maneuverability requirements for fighter aircraft has necessitated an extensive engineering development effort be directed towards inlet/engine compatibility. Inlet/engine compatibility must be assessed early in the aircraft development program to allow necessary inlet and engine design modifications to be defined and implemented at minimum cost impact. This early assessment of inlet/engine compatibility is determined by engine stability audits computed using inlet distortion levels from subscale inlet model data and engine sensitivities to inlet distortion. Therefore, the accuracy with which subscale inlet model distortion levels predict flight test vehicle distortion levels is a crucial element in assessing inlet/engine compatibility.

The primary goal of this distortion methodologies study was to determine if time variant distortion data taken from a subscale inlet model can predict peak distortion levels for a full scale flight test vehicle. The data base used to accomplish this goal was collected in separate programs by MCAIR and NASA/Dryden. Subscale and full scale wind tunnel data were collected by MCAIR during the F-15 development program, and flight test data were collected by NASA/Dryden during the NASA F-15 inlet/engine compatibility flight test program. This data base has a Mach number range of 0.4 to 2.5 and an angle of attack range from -10 degrees to +12 degrees.

The primary objectives accomplished in meeting the overall program goal were to determine the effects on peak distortion of: (1) Reynolds Number/scale, (2) engine presence and (3) frequency content. In addition, the capability of the P&WA stability audit system to predict engine stalls was evaluated, and the capability of Melick's procedure, Reference (1), to predict peak time variant distortion levels was evaluated. Using the Pratt and Whitney Aircraft distortion descriptor, K_{a_2}, the data indicate the following significant results for the F-15/F100 inlet/engine propulsion system.

- Peak time variant distortion from subscale inlet model wind tunnel tests are representative of full scale flight test distortion.
- The time variant pressure data of this study are random stationary data, thereby allowing valid statistical analyses to be conducted.
- The effect of the engine presence on total pressure recovery, peak time variant distortion and turbulence level is small but favorable.
- The Reynolds number/scale evaluation indicates a general trend of increasing total pressure recovery, decreasing peak time variant fan distortion and decreasing turbulence with increasing Reynolds number/scale.
- The frequency content evaluation indicates that peak time variant fan distortion and turbulence increase with increasing filter cutoff frequency for all of the data evaluated in this study.
- The capability of the Pratt & Whitney Aircraft stability audit system to predict engine stalls has been verified for both stall and non-stall flight test conditions.

- Predictions of peak distortion values using Melick's procedure are accurate to 11.3 percent average error for fourteen data points having nominal turbulence levels and are accurate to 20 percent average error (the maximum error approaches 40 percent) for eight data points having high turbulence levels.

APPENDIX J

STABILITY AUDITS

Presented herein are the remaining five flight points on which stability audits were conducted. As in the technical discussion section of Volume I, a set of figures is presented for each flight test condition audited. Instrumentation data traces, peak distortion selection procedures, fan inlet patterns audited and the stability audits are shown in Figures J-1 through J-18. The stability audit for each flight test condition is discussed below.

Stability Audit (Mach = 0.4, Altitude = 7,050m, WAT2 = 104.1%, I.D. = 1)

A fan induced stall during steady state augmentor operation with the third ramp actuator fully extended is illustrated in Figure J-1. An audit of the peak distortion just prior to stall from Figure J-2 indicates a negative 3.9 percent fan stall margin with a positive 16.4 percent HPC stall margin remaining as shown in Figure J-4. For this flight condition, the fan inlet pattern was not available for the peak distortion level for which a stability audit was conducted. Therefore, a representative pattern, which occurred slightly earlier in time (≈ 23 milliseconds) and had an equivalent distortion level was used and is shown in Figure J-3.

Stability Audit (Mach = 0.70, Altitude = 16,440m, WAT2 = 104.2%, I.D. = 4)

An augmentor blowout during steady state augmentor operation followed by augmentor reignition, which resulted in a fan induced stall with the third ramp actuator extended, is illustrated in Figure J-5. An audit of the peak distortion prior to surge, Figure J-6, indicates stable fan operation after the blowout but prior to augmentation reignition. Upon reignition a negative 26.5 percent fan stall margin and 12.3 percent positive HPC stall margin was determined as shown in Figure J-8. The augmentor blowout and reignition effects on the fan operating point were determined from fan discharge high response pressure traces.

Stability Audit (Mach = 0.92, Altitude = 16,390m, WAT2 = 104.5%, I.D. = 16)

An augmentor blowout followed immediately by an augmentor reignition induced fan stall is illustrated in Figure J-9. Prior to these anomalies, the engine was in steady state augmentor operation with the third ramp actuator extended. The peak distortion just prior to stall, Figure J-10, was audited and the results are shown in Figure J-12. The fan audit indicates stable operation until augmentor reignition occurs which resulted in a negative 18 percent fan stall margin. The corresponding HPC audit indicates a positive 12.5 percent stall margin remaining.

Stability Audit (Mach = 1.2, Altitude = 16,210m, WAT2 = 96.4%, I.D. = 35)

Traces of high response pressures and third ramp actuator position were not available for this event. However, a stall did occur during this event as confirmed by digital data. Audit results are shown in Figure J-15 and indicate a negative 9.2 percent fan stall margin and a positive 10.7 percent HPC stall margin remaining. These results concur with those at the same Mach Number but at Lower altitude (I.D. Number = 34) where the fan and HPC stall margin remaining were both more positive (-3.1 percent and +16.2 percent respectively) due to lower Reynolds Number effect. Based on these comparisons, it is concluded during this event.

Stability Audit (Mach = 2.0, Altitude = 19,030m, WAT2 = 77.0%, I.D. = 57)

This stability audit was for non-stall engine operation at supersonic conditions with steady state augmentor operation and the inlet third ramp scheduled automatically. High response pressure and inlet third ramp actuator position traces were similar to those for Data Point 44 and have not been included. The peak distortion level of Figure J-16 was audited and the results are shown in Figure J-18. The audits indicated a positive 15.4 percent fan stall margin remaining and a positive 15.7 percent HPC stall margin remaining.

DATA POINT I.D. NO.	MODEL SCALE	M_0	α (DEG)	β (DEG)	ρ (DEG)	Δ3 (DEG)	BYPASS*	% WAT2	RE NO. $\times 10^{-6}$	ANALYSIS TIME (SEC)	PART–POINT**
1	FLT	0.4	16.4	−0.3	6.9	27.6	C	104.1	1.44	0.6	422-4
2	FLT	0.59	13.9	0.9	7.0	26.6	C	102.[illegible]	2.04	0.6	417-5
3	↓	0.52	10.0	0.7	↓	27.6	↓	107.1	1.33	0.6	417-4
4	↓	0.69	11.5	1.0	↓	26.5	↓	104.2	0.84	0.6	417-2
5	1/6th	0.60	−10.0	10.0	−3.0	10.6	C	97.2	0.43	0.144	164-1
6	1/6th	0.60	−10.0	10.0	−3.0	10.6	C	90.2	0.43	0.144	164-3
7	FLT	0.69	−8.4	10.6	0.6	10.5	C	101.2	1.40	0.88	421-10
8	1/3th	0.60	4.0	0	7.0	10.6	C	76.6	0.43	0.181	112-7
9	1/6th	0.60	4.0	0	7.0	10.6	C	108.6	0.43	0.181	112-5
10	FSE	0.60	4.0	0	5.2	10.0	C	97.7	3.41	1.110	116-2
11	FLT	0.67	4.3	0.7	6.9	11.1	C	94.4	3.58	0.72	424-2
12	↓	0.69	3.4	0.7	6.9	11.1	↓	74.1	3.68	0.76	425-6
13	↓	0.59	4.6	1.2	7.0	11.1	↓	107.9	1.74	0.62	412-2
14	↓	0.60	4.6	0.6	6.9	11.0	↓	76.2	1.66	1.11	424-11
15	FLT	0.85	8.8	−0.5	7.0	27.6	C	104.2	2.21	0.60	417-3
16	FLT	0.92	5.6	0.6	7.0	26.6	C	104.5	1.04	0.60	417-1
17	1/6th	0.90	−10.0	10.0	−3.0	10.6	C	70.2	0.34	0.113	157-7
18	1/6th	0.90	−10.0	10.0	−3.0	10.6	C	106.3	0.34	0.113	157-5
19	FLT	0.94	−8.9	10.2	1.0	10.5	C	107.1	1.6	0.69	421-14
20	FSE	0.90	−4.0	0	−1.0	8.2	C	97.8	3.64	1.990	102-2
21	FLT	0.90	−2.8	−0.2	−1.2	8.7	C	97.5	3.25	1.23	424-10
22	FLT	0.93	−3.3	0	−1.2	8.6	C	104.8	1.17	1.99	425-3
23	1/6th	0.90	4.0	0	7.0	10.6	C	76.8	0.34	0.369	67-9
24	1/6th	0.90	4.0	0	7.0	10.6	C	104.3	0.34	0.369	67-7
25	FSE	0.90	4.0	0	7.3	10.4	C	97.7	3.62	2.260	126-2
26	FLT	0.92	4.6	0.7	6.0	11.0	C	96.2	3.47	0.89	420-9
27	↓	0.91	5.2	0.5	6.9	11.1	↓	99.1	3.28	1.18	422-2
28	↓	0.92	4.2	0.1	7.0	11.0	↓	76.1	2.47	1.34	421-5
29	↓	0.90	4.1	0.5	6.9	11.1	↓	98.6	2.43	1.46	424-9
30	↓	0.90	5.1	0.1	7.0	11.0	↓	105.7	2.42	0.69	421-4
31	↓	0.90	3.5	0.2	7.0	11.0	↓	77.5	1.78	2.26	421-6
32	↓	0.90	5.2	−0.1	7.0	11.0	↓	100.1	1.79	0.70	421-7
33	↓	0.94	4.3	0.2	7.0	11.1	↓	105.6	1.89	1.06	421-8

*C = Closed

**For flight test, these data are flight-run numbers

GP79-0323-8

TABLE J-1
DATA MATRIX

ORIGINAL PAGE IS
OF POOR QUALITY

DATA POINT I.D. NO.	MODEL SCALE	M_0	α (DEG)	β (DEG)	ρ (DEG)	Δ3 (DEG)	BYPASS*	% WAT2	RE NO. x 10^{-6}	ANALYSIS TIME (SEC)	PART–POINT**
34	FLT	1.21	1.5	0	6.0	27.6	C	98.3	2.97	0.60	423-4
35	FLT	1.24	3.0	0.8	6.7	27.6	C	96.4	1.52	0.60	423-3
36	1/6th	1.2	10.0	0	7.0	10.6	C	76.6	0.45	0.198	131-7
37	1/6th	1.2	10.0	0	7.0	10.6	C	107.9	0.45	0.198	131-5
38	FLT	1.18	7.7	0.3	7.0	11.0	C	74.0	3.22	1.21	424-12
39	↓	1.2	7.4	−0.1	7.1	11.1	↓	94.4	3.35	1.19	424-13
40	↓	1.17	10.6	0.0	7.0	11.0	↓	103.4	1.40	0.60	421-17
41	FLT	1.54	1.5	0	−1.4	27.0	Auto	95.4	2.17	0.60	424-6
42	1/6th	1.6	−4.0	0	−2.0	13.5	C	87.3	0.21	0.106	206-9
43	1/6th	1.6	−4.0	0	−2.0	13.5	C	96.9	0.21	0.106	206-5
44	FLT	1.57	−3.6	0.7	−2.3	13.7	C	89.3	1.46	0.65	414-2
45	1/6th	1.8	−2.0	0	−3.0	17.4	C	80.5	0.22	0.210	15-9
46	1/6th	1.8	−2.0	0	−3.0	17.4	C	91.0	0.22	0.201	15-5
47	FLT	1.75	−2.6	0.4	−2.2	16.7	C	80.7	1.41	1.23	415-1
48	FSCP	1.8	−2.0	0	−3.0	18.7	C	75.1	1.45	0.680	353-15
49	↓	↓	−2.0	↓	−3.0	↓	↓	82.2	1.45	0.680	353-5
50	↓	↓	−2.0	↓	−3.0	↓	↓	85.4	1.44	0.680	353-12
51	FSE	1.8	−2.0	0	−2.9	18.6	C	80.6	1.46	0.680	523-2
52	FSE	1.8	−2.0	0	−2.9	18.6	C	79.8	1.46	0.680	525-4
53	FLT	1.81	−2.3	0.2	−2.9	18.2	C	78.9	1.53	0.680	416-1
54	FSCP	1.8	4.0	0	2.5	18.7	C	79.9	1.45	2.800	355-8
55	FSE	1.8	4.0	0	2.5	18.7	C	80.8	1.46	2.800	528-2
56	FSE	1.8	4.0	0	2.5	18.7	C	79.7	1.46	2.800	529-4
57	FLT	2.0	2.5	0.2	2.3	20.9	Auto	77.0	1.72	2.800	425-2

*C = Closed
**For flight test, these data are flight-run numbers

GP78-0323-8

TABLE J-1 (Continued)
DATA MATRIX

ORIGINAL PAGE IS
OF POOR QUALITY

DATA POINT I.D. NO.	MODEL SCALE	M_0	α (DEG)	β (DEG)	ρ (DEG)	Δ3 (DEG)	BYPASS*	% WAT2	RE NO. x 10^{-6}	ANALYSIS TIME (SEC)	PART–POINT**
58	1/6th	2.2	−2.0	0	−4.0	22.5	C	68.6	0.22	0.100	250-7
59	FSCP	2.2	−2.0	0	−4.0	22.5	C	69.2	1.48	0.600	411-6
60	1/6th	2.2	−2.0	0	−4.0	25.0	O	65.0	0.22	0.100	249-5
61	1/6th	2.2	−2.0	0	−4.0	25.0	O	52.9	0.22	0.100	249-9
62	FSCP	2.2	−2.0	0	−4.0	25.0	O	61.7	1.48	0.600	385-5
63	FSCP	2.2	−2.0	0	−4.0	25.0	O	62.3	1.48	0.600	385-2
64	FSE	2.2	−2.0	0	−4.0	24.8	P	60.2	1.27	0.600	542-2
65	FSE	2.2	−2.0	0	−4.0	24.8	P	60.5	1.27	0.600	543-4
66	1/6th	2.2	0	0	−2.0	22.5	C	69.3	0.22	0.106	184-7
67	1/6th	2.2	0	0	−2.0	22.5	C	75.4	0.22	0.106	184-5
68	FSCP	2.2	0	0	−2.0	22.5	C	73.6	1.47	0.650	413-9
69	FSCP	2.2	0	0	−2.0	22.5	C	68.3	1.47	0.650	413-12
70	FLT	2.2	0.1	0.2	−2.2	22.9	C	73.0	2.34	0.650	425-1
71	FSCP	2.2	4.0	0	0.0	25.0	O	60.7	1.48	0.600	382-3
72	FSE	2.2	4.0	0	1.0	25.0	O	59.2	1.28	0.600	545-2
73	FSE	2.2	4.0	0	1.0	25.0	O	58.2	1.27	0.600	546-4
74	1/6th	2.2	12.0	0	6.0	25.0	O	47.3	0.22	0.100	252-9
75	1/6th	2.2	12.0	0	6.0	25.0	O	65.0	0.22	0.100	252-5
76	FSCP	2.2	12.0	0	6.8	25.0	O	60.8	1.48	0.600	384-2
77	FSE	2.2	11.0	0	6.8	24.8	O	59.0	1.28	0.600	548-3
78	FSE	2.2	11.0	0	6.8	24.8	P	59.8	1.27	0.600	549-8
79	1/6th	2.5	0	0	−4.0	26.0	O	63.1	0.21	0.100	227-7
80	1/6th	2.5	0	0	−4.0	26.0	O	68.2	0.21	0.100	227-5
81	FSCP	2.5	0	0	−4.0	26.0	O	62.8	1.28	0.600	465-8
82	FSCP	2.5	0	0	−4.0	26.0	O	68.9	1.28	0.600	465-5

*O = Open, C = Closed, P = Partial

**For flight test, these data are flight-run numbers

GP78-0323-10

TABLE J-1 (Concluded)
DATA MATRIX

ORIGINAL PAGE IS
OF POOR QUALITY

TIME HISTORIES OF HIGH RESPONSE PRESSURE PROBE DATA

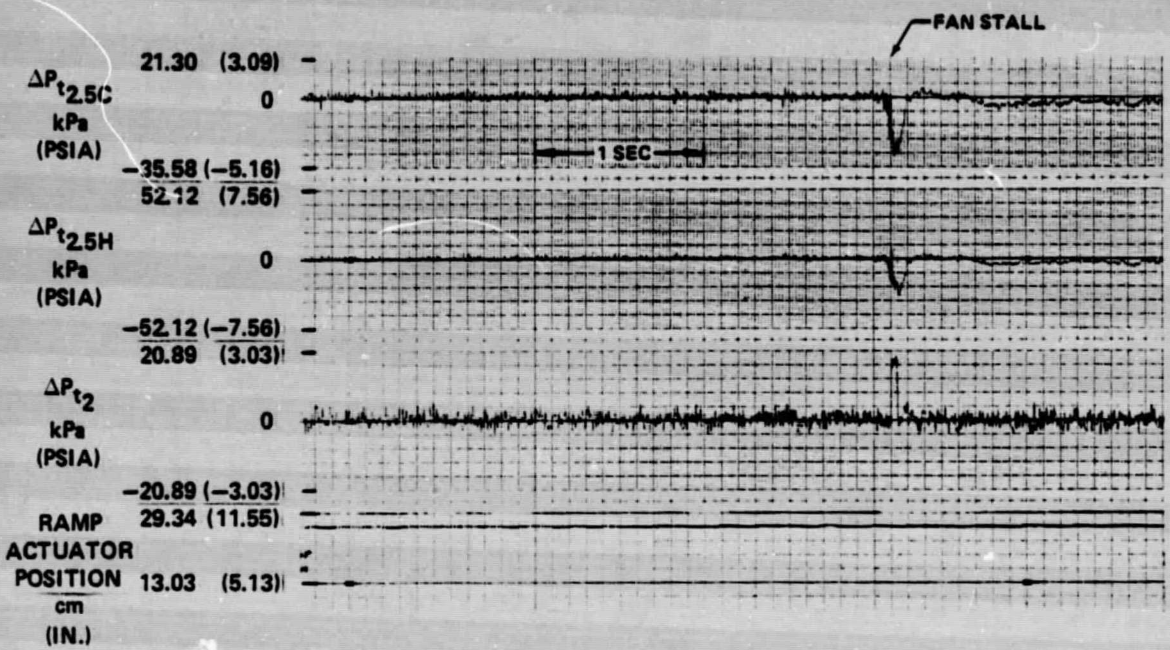

FIGURE J-1
STABILITY AUDIT ANALYSIS PLOTS
Mach 0.4 α = 16.4 β = —0.8 ρ = 6.9
Δ_3= 27.6 WAT2 = 104.1 Bypass = 0 I.D. Number = 1

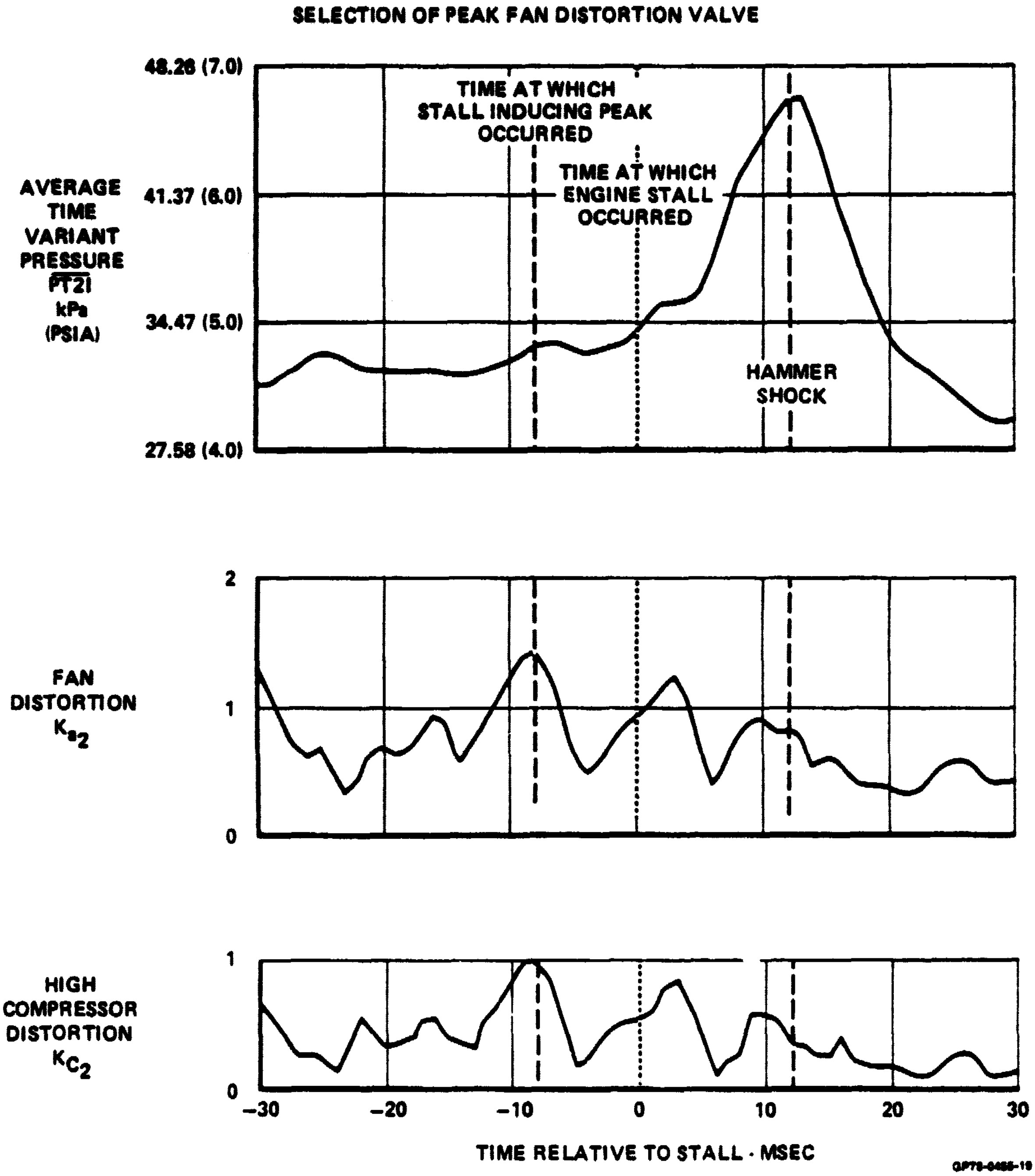

FIGURE J-2
STABILITY AUDIT ANALYSIS PLOTS
Mach 0.4 α = 16.4 β = −0.8 ρ = 6.9
Δ_3 = 27.6 WAT2 = 104.1 Bypass = 0 I.D. Number = 1

ORIGINAL PAGE IS
OF POOR QUALITY

TOTAL PRESSURE CONTOUR AT PEAK FAN DISTORTION

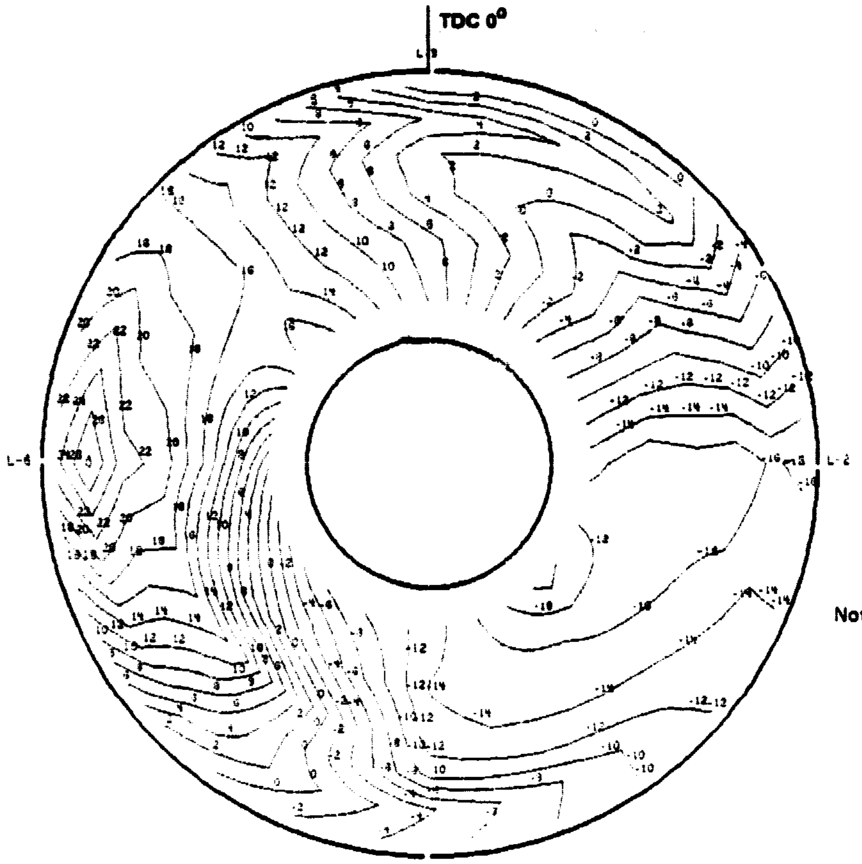

K_{A2} = 1.3

K_{C2} = 0.9

$\frac{\Delta P}{P}\left(\frac{MAX - MIN}{AVG}\right) = 50.0\%$

Note: Representative pattern, not actual pattern audited

GP78-0455-39

FIGURE J-3

STABILITY AUDIT ANALYSIS PLOTS

Mach 0.4 α = 16.4 β = —0.8 ρ = 6.9

Δ_3 = 27.6 WAT2 = 104.1 Bypass = 0 I.D. Number = 1

Legend

Surge Pressure Ratio
- A - Highest available
- A to B - Reynolds no. loss
- B to C - Engine to engine variation
- C to D - Distortion loss

Operating Pressure Ratio
- 1 - Installed match point
- 2 - Distortion rematch
- 3 - Augmentor anomaly

FAN AND COMPRESSOR MAPS FOR THE STABILITY AUDITS

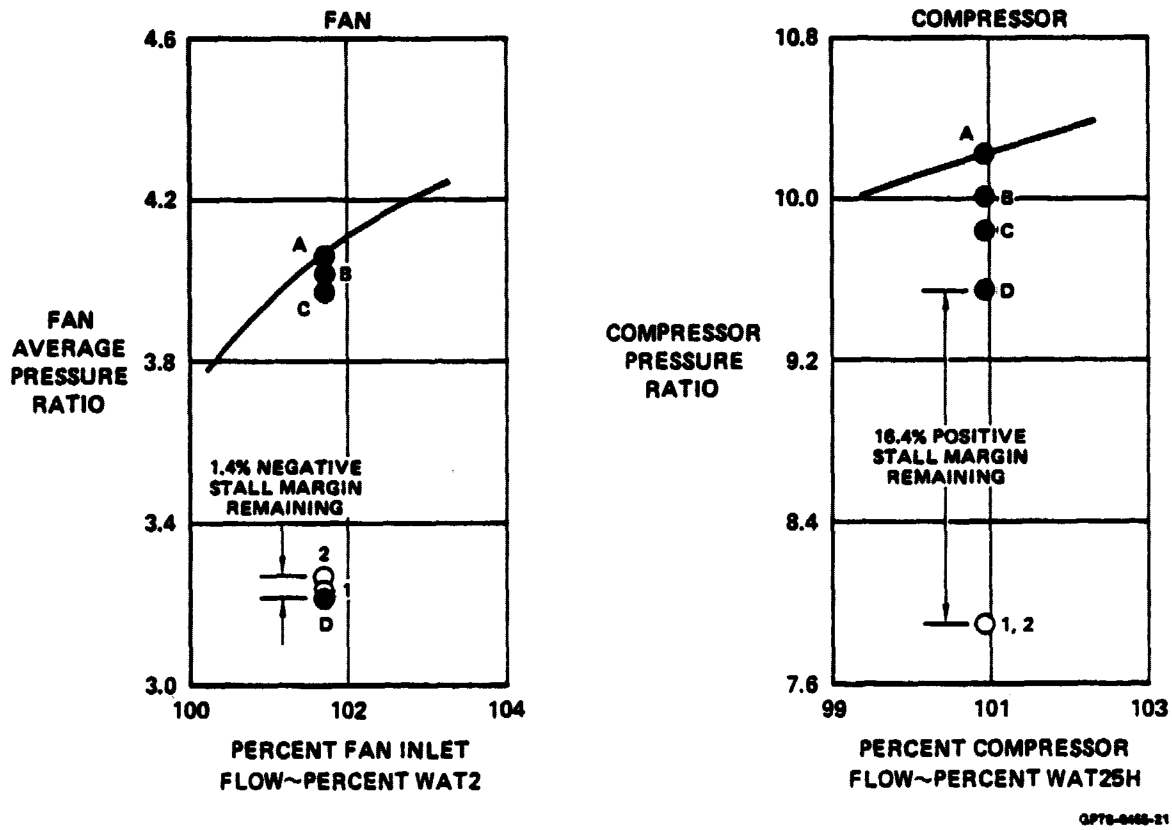

FIGURE J-4
STABILITY AUDIT ANALYSIS PLOTS
Mach 0.4 α = 16.4 β = —0.8 ρ = 6.9
Δ_3 = 27.6 WAT2 = 104.1 Bypass = 0 I.D. Number = 1

ORIGINAL PAGE IS
OF POOR QUALITY

TIME HISTORIES OF HIGH RESPONSE PRESSURE PROBE DATA

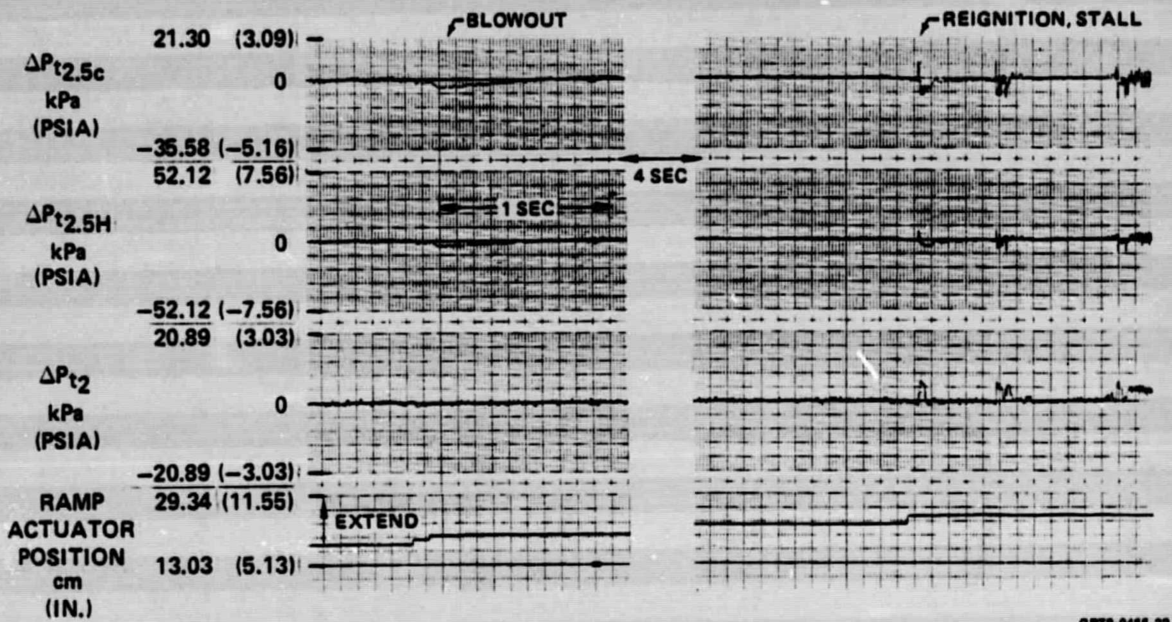

FIGURE J-5
STABILITY AUDIT ANALYSIS PLOTS
Mach 0.61 α = 11.5 β = 1.0 ρ = 7.0
Δ_3 = 26.5 WAT2 = 104.2 Bypass = 0 I.D. Number = 4

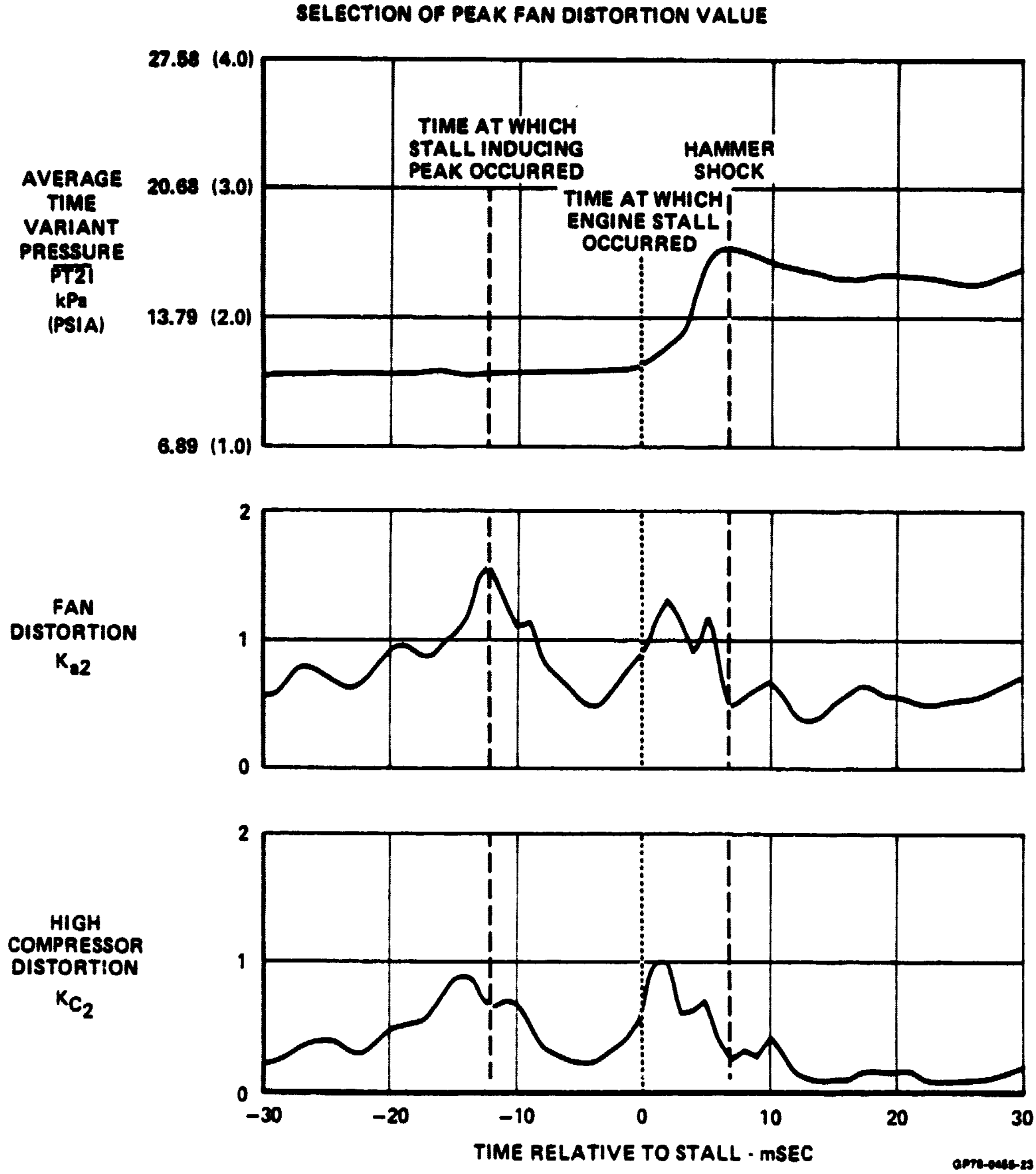

FIGURE J-6
STABILITY AUDIT ANALYSIS PLOTS
Mach 0.61 α = 11.5 β = 1.0 ρ = 7.0
Δ_3 = 26.5 WAT2 = 104.2 Bypass = 0 I.D. Number = 4

ORIGINAL PAGE IS
OF POOR QUALITY

TOTAL PRESSURE CONTOUR AT PEAK FAN DISTORTION

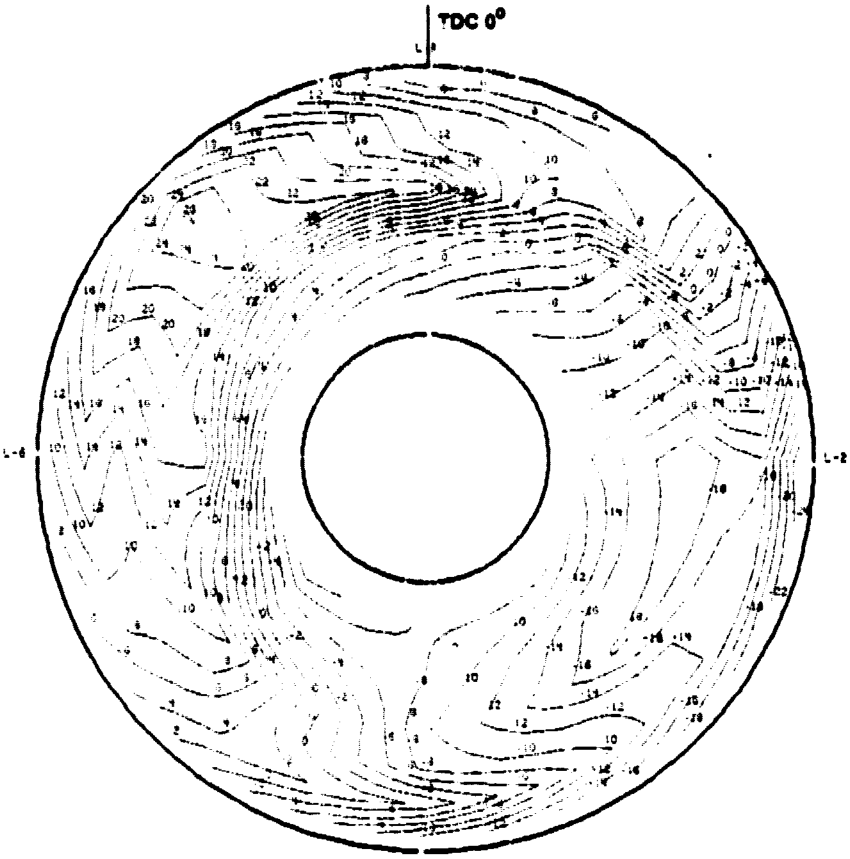

$K_{A2} = 1.6$
$K_{C2} = 0.70$
$\frac{\Delta P}{P}\left(\frac{MAX-MIN}{AVG}\right) = 51.6\%$

GP79-0486-24

FIGURE J-7
STABILITY AUDIT ANALYSIS PLOTS
Mach 0.61 $\alpha = 11.5$ $\beta = 1.0$ $\rho = 7.0$
$\perp_3 = 26.5$ WAT2 = 104.2 Bypass = 0 I.D. Number = 4

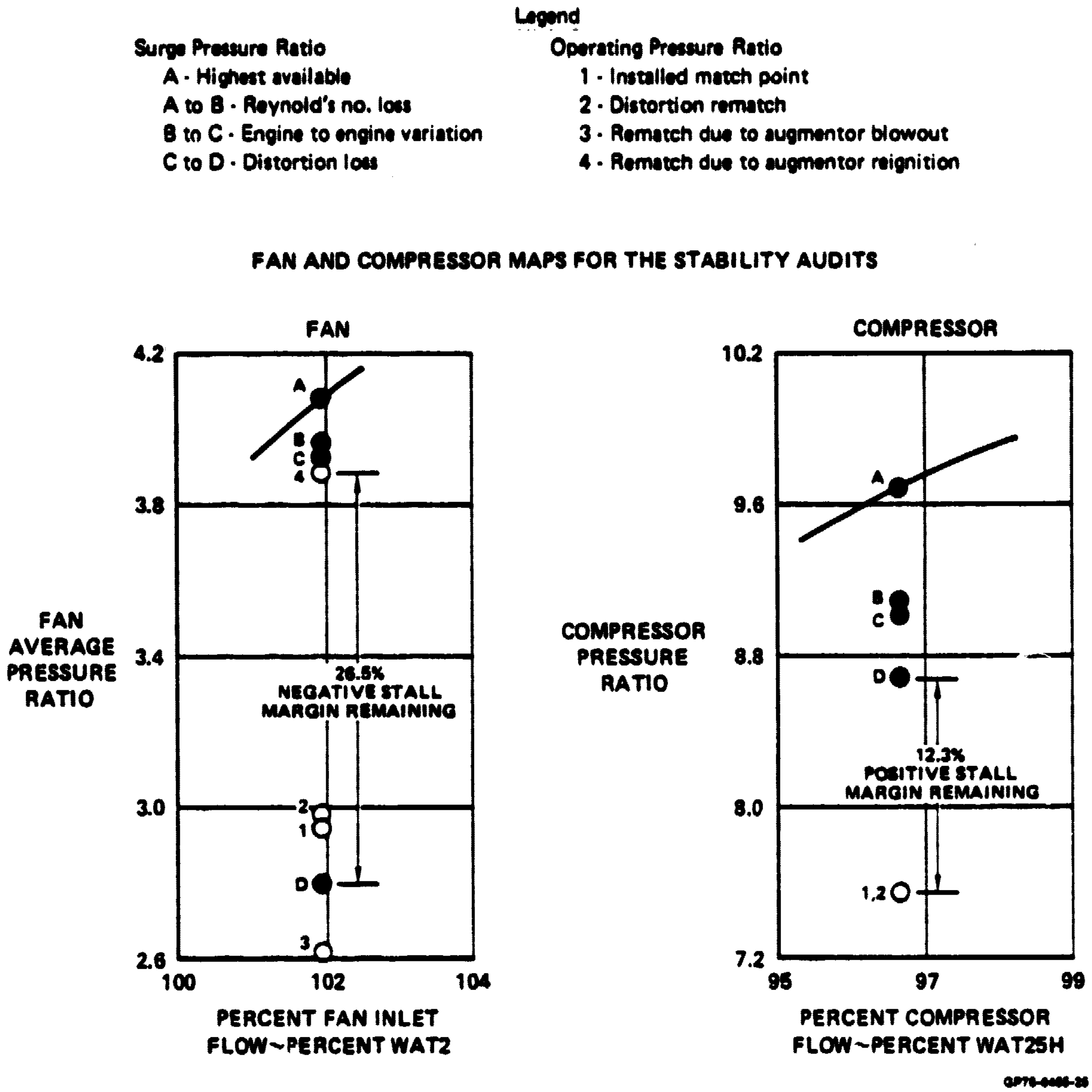

FIGURE J-8
STABILITY AUDIT ANALYSIS PLOTS
Mach 0.61 α = 11.5 β = 1.0 ρ = 7.0
Δ_3 = 26.5 WAT2 = 104.2 Bypass = 0 I.D. Number = 4

ORIGINAL PAGE IS
OF POOR QUALITY

TIME HISTORIES OF HIGH RESPONSE PRESSURE PROBE DATA

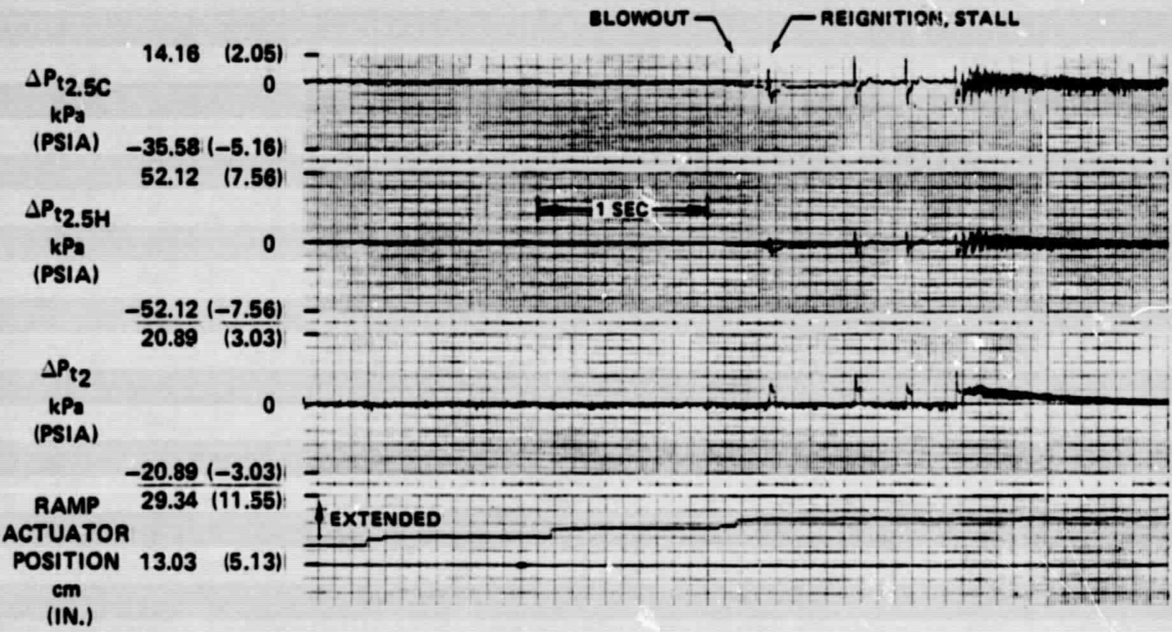

FIGURE J-9
STABILITY AUDIT ANALYSIS PLOTS
Mach 0.92 α = 5.6 β = 0.6 ρ = 7.0
Δ_3 = 26.6 WAT2 = 104.5 Bypass = 0 I.D. Number = 16

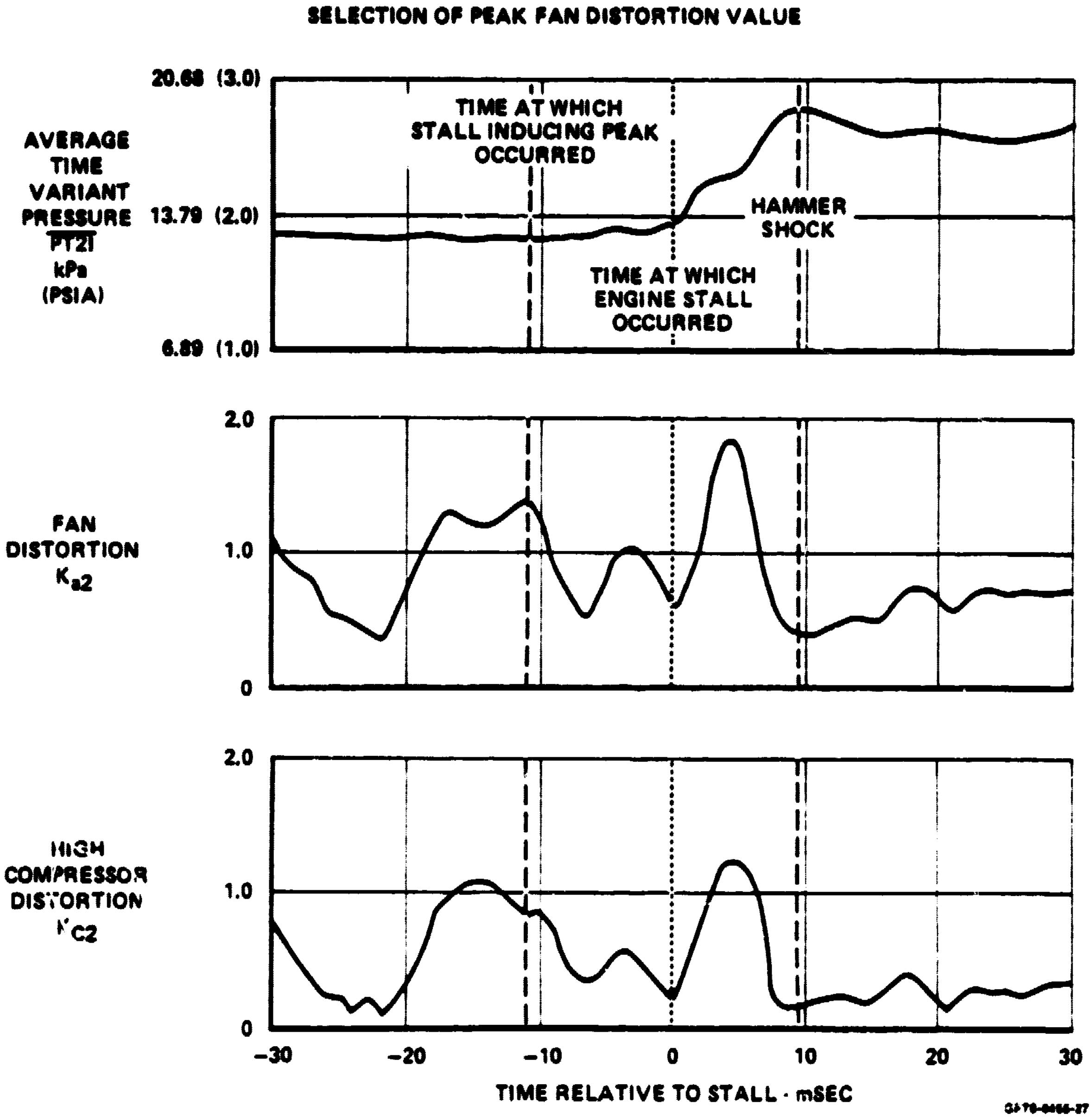

FIGURE J-10
STABILITY AUDIT ANALYSIS PLOTS
Mach 0.92 α = 5.6 β = 0.6 ρ = 7.0
Δ_3= 26.6 WAT2 = 104.5 Bypass = 0 I.D. Number = 16

ORIGINAL PAGE IS
OF POOR QUALITY

TOTAL PRESSURE CONTOUR AT PEAK FAN DISTORTION

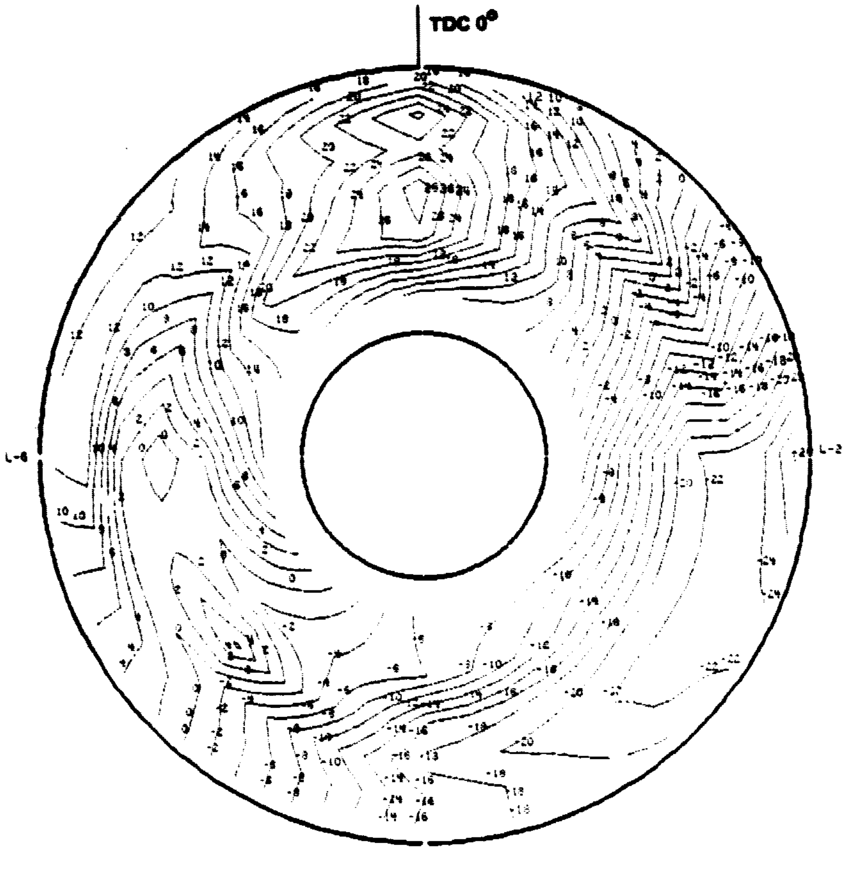

$K_{A2} = 1.4$

$K_{C2} = 0.85$

$\frac{\Delta P}{P} \left(\frac{\text{MAX - MIN}}{\text{AVG}} \right) = 57.6\%$

GP78-0456-28

FIGURE J-11
STABILITY AUDIT ANALYSIS PLOTS
Mach 0.92 $\alpha = 5.6$ $\beta = 0.6$ $\rho = 7.0$
$\Delta_3 = 26.6$ WAT2 = 104.5 Bypass = 0 I.D. Number = 16

Legend

Surge Pressure Ratio
- A - Highest available
- A to B - Reynold's no. loss
- B to C - Engine to engine variation
- C to D - Distortion loss

Operating Pressure Ratio
- 1 - Installed match point
- 2 - Distortion rematch
- 3 - Rematch due to augmentor blowout
- 4 - Rematch due to augmentor reignition

FAN AND COMPRESSOR MAPS FOR THE STABILITY AUDITS

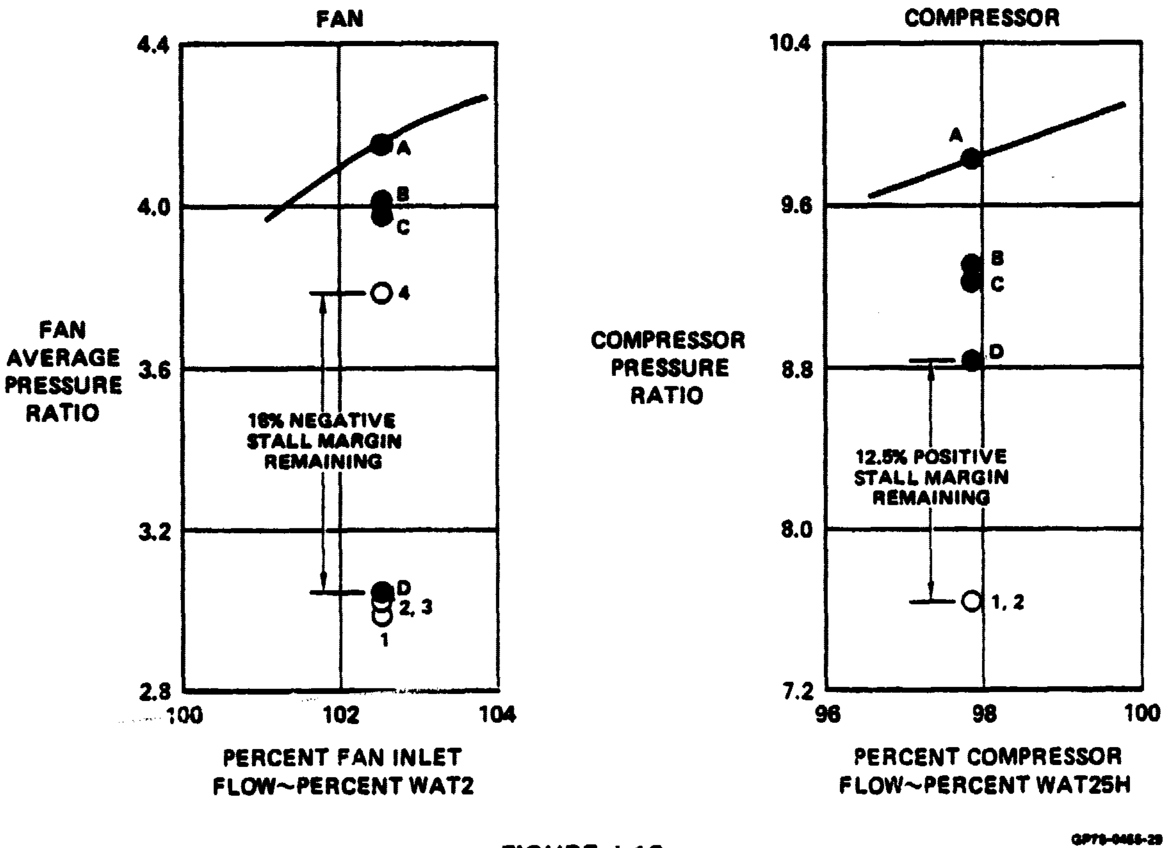

FIGURE J-12
STABILITY AUDIT ANALYSIS PLOTS
Mach 0.92 α = 5.6 β = 0.6 ρ = 7.0
Δ_3 = 26.6 WAT2 = 104.5 Bypass = 0 I.D. Number = 16

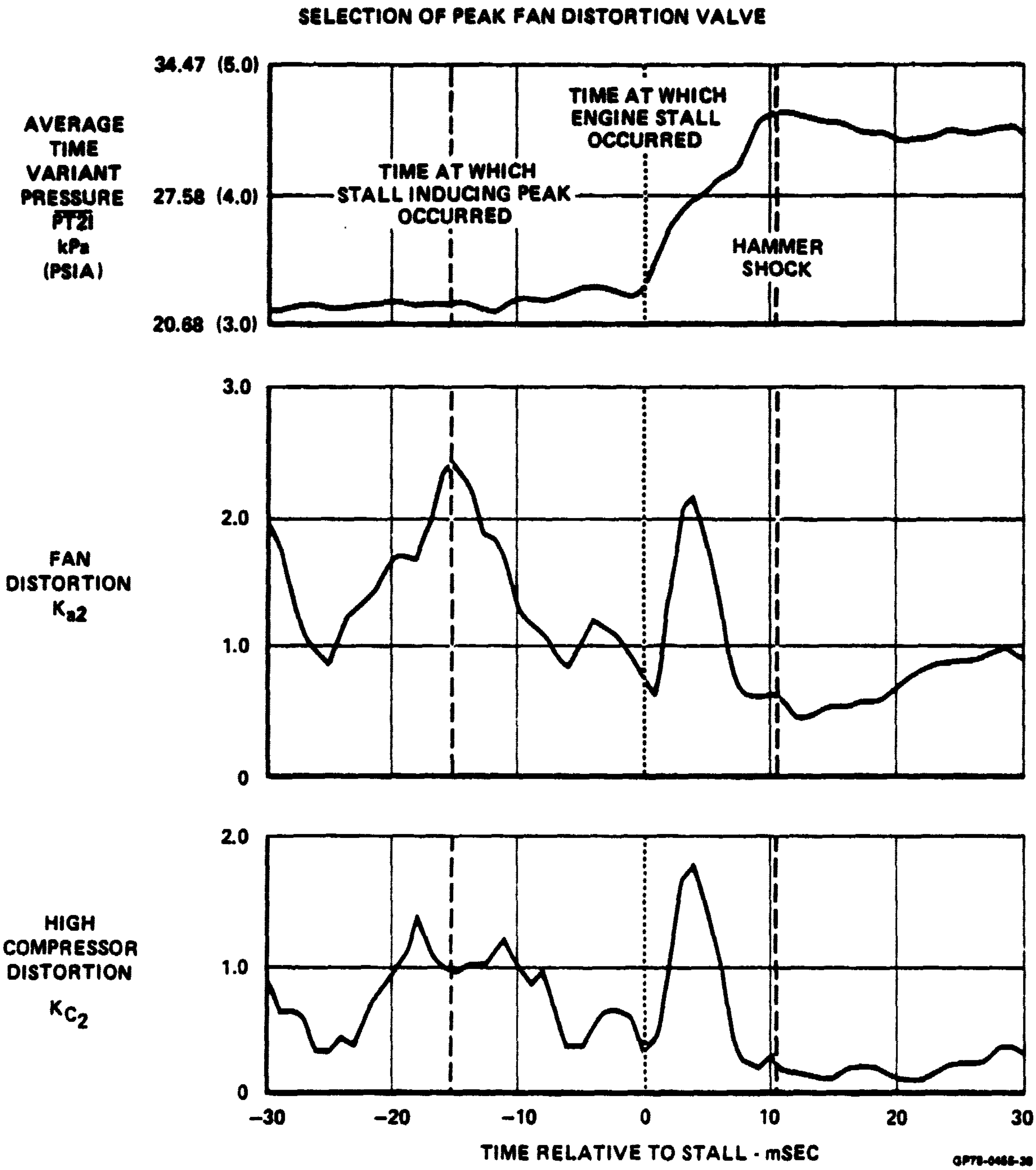

FIGURE J-13
STABILITY AUDIT ANALYSIS PLOTS
Mach 1.24 $\alpha = 3.0$ $\beta = 0$ $\rho = 6.7$
$\Delta_3 = 27.6$ WAT2 = 96.4% Bypass = 0 I.D. Number = 35

ORIGINAL PAGE IS
OF POOR QUALITY

TOTAL PRESSURE CONTOUR AT PEAK FAN DISTORTION

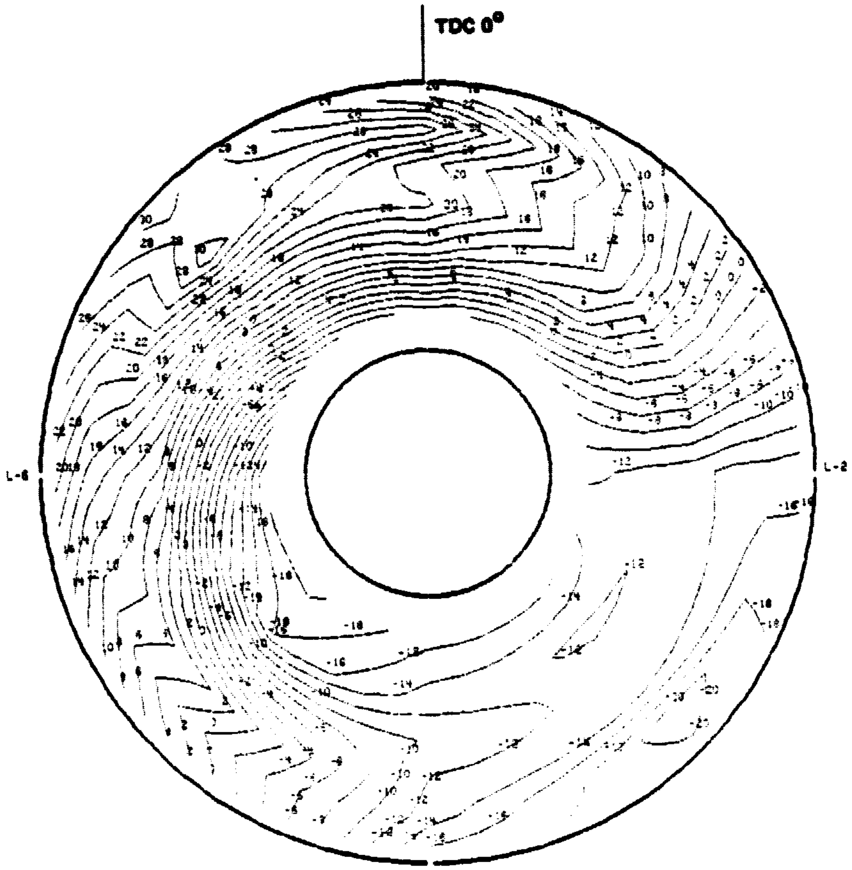

$K_{A2} = 2.3$
$K_{C2} = 0.93$
$\frac{\Delta P}{P} \left(\frac{MAX - MIN}{AVG}\right) = 52.4\%$

FIGURE J-14
STABILITY AUDIT ANALYSIS PLOTS
Mach 1.24 $\alpha = 3.0$ $\beta = 0$ $\rho = 6.7$
$\Delta_3 = 27.6$ WAT2 = 96.4% Bypass = 0 I.D. Number = 35

Legend

Surge Pressure Ratio	Operating Pressure Ratio
A - Highest available	1 - Installed match point
A to B - Reynold's no. loss	2 - Distortion rematch
B to C - Engine to engine variation	3 - Augmentor anomaly
C to D - Distortion loss	

FAN AND COMPRESSOR MAPS FOR THE STABILITY AUDITS

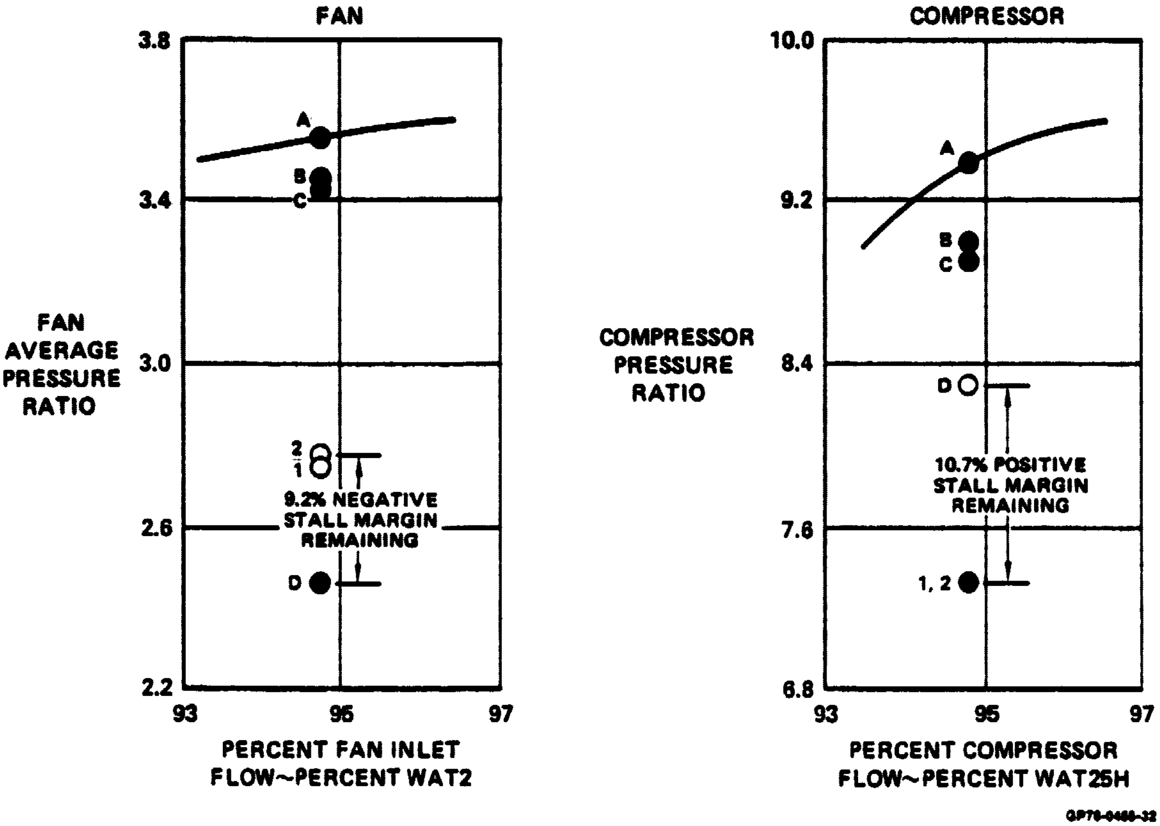

FIGURE J-15
STABILITY AUDIT ANALYSIS PLOTS
Mach 1.24 $\alpha = 3.0$ $\beta = 0$ $\rho = 6.7$
$\lambda_3 = 27.6$ WAT2 = 96.4% Bypass = 0 I.D. Number = 35

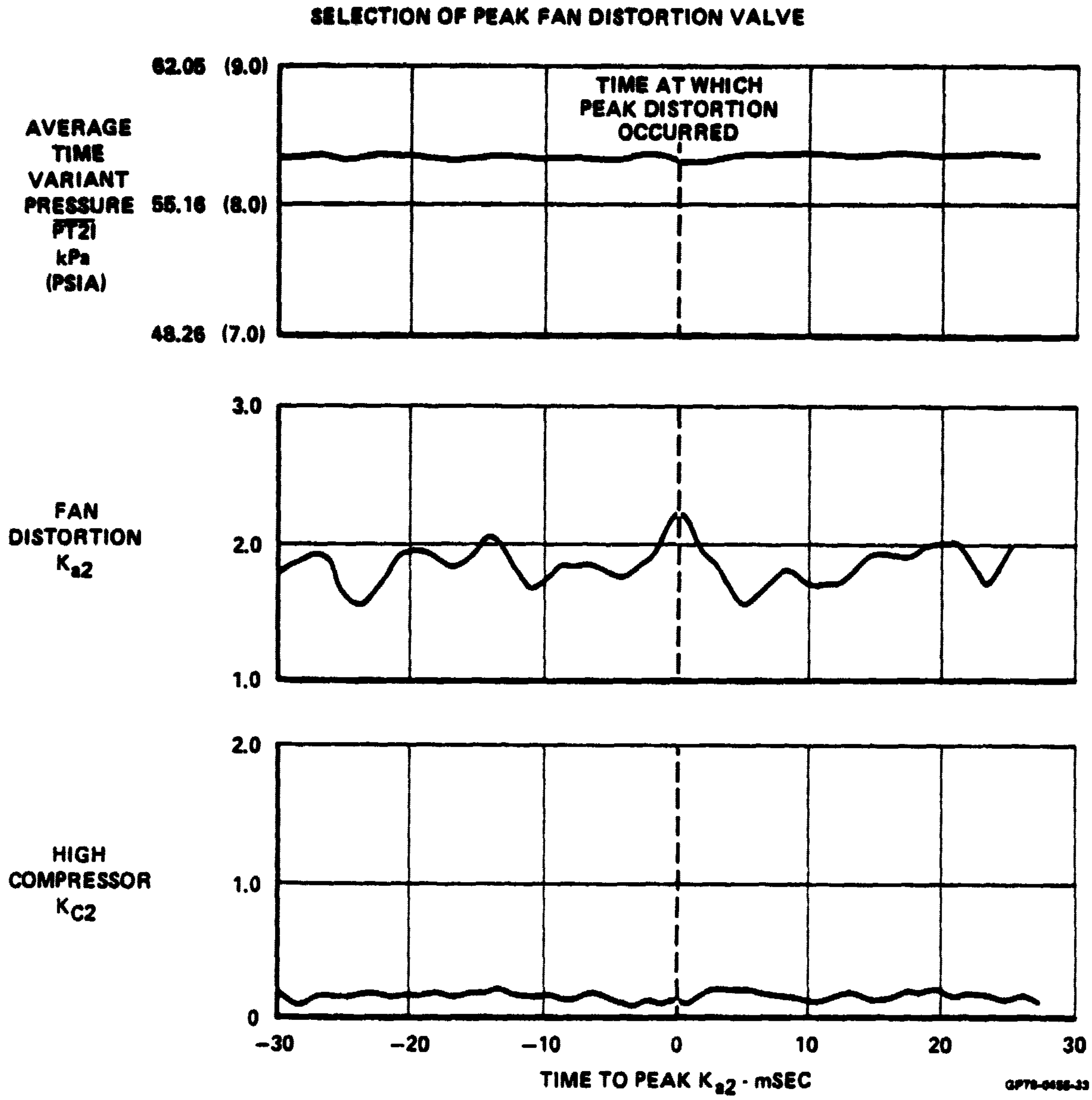

FIGURE J-16
STABILITY AUDIT ANALYSIS PLOTS
Mach 2.0 α = 2.5 β = 0.2 ρ = 2.3
Δ_3 = 20.9 WAT2 = 77.0 Bypass = Auto I.D. Number = 57

ORIGINAL PAGE IS
OF POOR QUALITY

TOTAL PRESSURE CONTOUR AT PEAK FAN DISTORTION

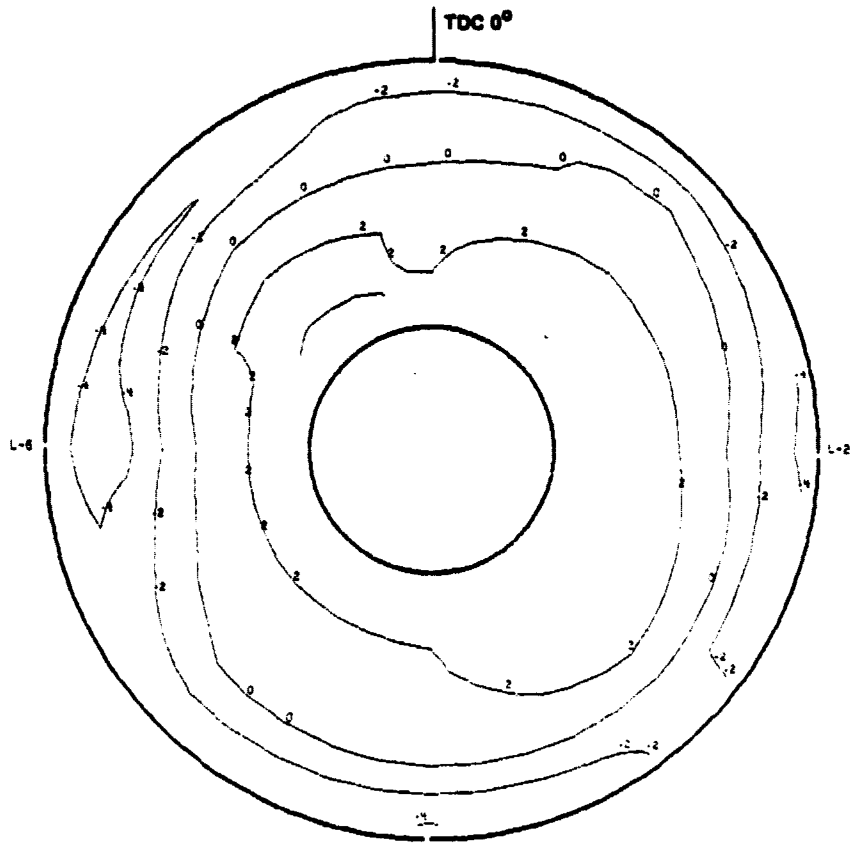

$K_{A2} = 2.0$
$K_{C2} = 0.14$
$\frac{\Delta P}{P} \left(\frac{MAX - MIN}{AVG}\right) = 8.9\%$

GP78-0458-34

FIGURE J-17
STABILITY AUDIT ANALYSIS PLOTS
Mach 2.0 $\alpha = 2.5$ $\beta = 0.2$ $\rho = 2.3$
$\Delta_3 = 20.9$ WAT2 = 77.0 Bypass = Auto I.D. Number = 57

Legend

Surge Pressure Ratio
- A - Highest available
- A to B - Reynold's no. loss1
- B to C - Engine to engine variation
- C to D - Distortion loss

Operating Pressure Ratio
- 1 - Installed match point
- 2 - Distortion rematch
- 3 - Augmentor anomaly

FAN AND COMPRESSOR MAPS FOR THE STABILITY AUDITS

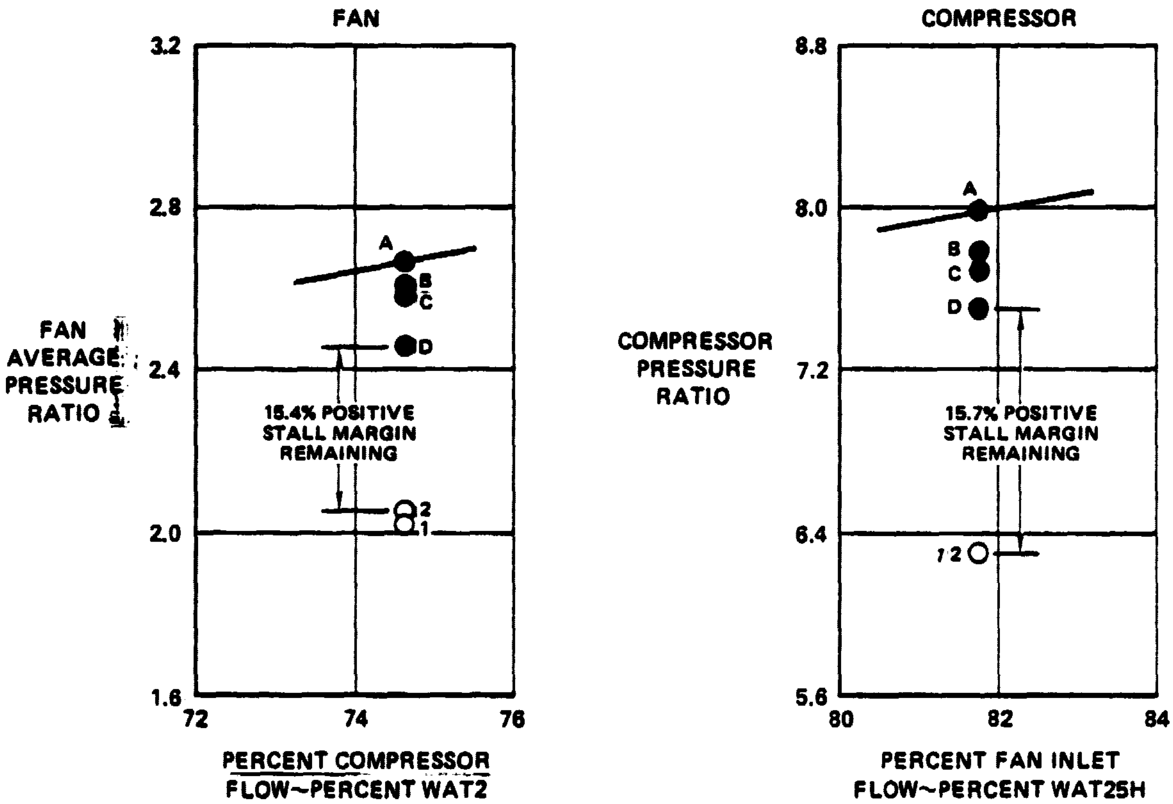

FIGURE J-18
STABILITY AUDIT ANALYSIS PLOTS
Mach 2.0 $\alpha = 2.5$ $\beta = 0.2$ $\rho = 2.3$
$\Delta_3 = 20.9$ WAT2 = 77.0 Bypass = Auto I.D. Number 57